AGU PUBLICATIONS

Geophysical Research Letters

RESEARCH LETTER

10.1002/2016GL071670

Key Points:

- Annual Landsat-derived channel masks of the Ucayali River over 31 years show planform responses to cutoffs
- For all 13 analyzed cutoffs the downstream extent of cutoff influence scaled with the net length of removed reach
- Results provide the first evidence of cutoff avalanching dynamics in meandering rivers

Supporting Information:

- Supporting Information S1

Correspondence to:
J. Schwenk,
jonschwenk@gmail.com

Citation:
Schwenk, J., and E. Foufoula-Georgiou (2016), Meander cutoffs nonlocally accelerate upstream and downstream migration and channel widening, *Geophys. Res. Lett.*, *43*, 12,437–12,445, doi:10.1002/2016GL071670.

Received 20 OCT 2016
Accepted 12 DEC 2016
Accepted article online 14 DEC 2016
Published online 30 DEC 2016

Meander cutoffs nonlocally accelerate upstream and downstream migration and channel widening

Jon Schwenk[1,2] and **Efi Foufoula-Georgiou**[2]

[1]Department of Civil, Environmental and Geo-Engineering and Saint Anthony Falls Laboratory, University of Minnesota, Twin Cities, Minneapolis, Minnesota, USA, [2]Department of Civil and Environmental Engineering, University of California, Irvine, California, USA

Abstract The hydrologic and sediment dynamics within and near cutoffs have long been studied, establishing them as effective agents of rapid local geomorphic change. However, the morphodynamic impact of individual cutoffs at the reachwide scale remains unknown, mainly due to insufficient observations of channel adjustments over large areal extents and at high temporal frequency. Here we show via annually resolved, Landsat-derived channel masks of the dynamic meandering Ucayali River in Peru that cutoffs act as perturbations that nonlocally accelerate river migration and drive channel widening both upstream and downstream of the cutoff locations. By tracking planform changes of individual meander bends near cutoffs, we find that the downstream distance of cutoff influence scales linearly with the length of the removed reach. The discovery of nonlocal cutoff influence supports the hypothesis of "avalanche"-type behavior in meander cutoff dynamics and presents new challenges in modeling and prediction of rivers' self-adjusting responses to perturbations.

1. Introduction

Meander cutoffs play a vital role in river morphodynamics by increasing local channel slope, decreasing river sinuosity, and reducing floodplain access. Unlike channel adjustments of width, depth, and length, which are typically spatially and temporally continuous, cutoffs are uniquely episodic by removing significant reaches from a river over short times. Over long time scales, cutoffs may influence meander migration rates through the creation of oxbow lakes that augment floodplain resistance heterogeneity. Oxbow lakes form "plugs" through the consolidation of silt, clay, and organic matter that increase local resistance to erosion and impede or confine meander migration [*Fisk et al.*, 1949; *Hudson and Kesel*, 2000]. On the other hand, oxbow lakes may also promote meander migration if the migrating channel revisits the oxbow before plugs have formed [*Schwendel et al.*, 2015]. A study of over 90 years of migration observations along the Sacramento River determined that cutoffs alone accounted for nearly 20% of the total channel migration [*Micheli and Larsen*, 2011].

Over shorter time scales, cutoffs act as "shot" perturbations [*Camporeale et al.*, 2008] to river morphodynamics by increasing the bed slope and stream power both upstream and downstream [*Biedenharn et al.*, 2000; *Hooke*, 2004; *Jugaru Tiron et al.*, 2009], injecting downstream pulses of sediment excavated from the floodplain during chute channel formation [*Fuller et al.*, 2003; *Zinger et al.*, 2011], and substantially altering the local channel planform and hydrodynamics [*Hooke*, 2004; *Zinger et al.*, 2013]. Considerable attention has been given to local cutoff-induced channel response immediately adjacent to and within cutoffs [*Hooke*, 1995; *Fuller et al.*, 2003; *Zinger et al.*, 2011, 2013] as well as factors controlling their occurrence [*Grenfell et al.*, 2014; *Eekhout and Hoitink*, 2015; *Słowik*, 2016]. However, the spatial and temporal extents to which cutoff perturbations induce nonlocal morphologic change remain unknown, largely due to difficulties of observing morphodynamics over sufficiently large spatial scales and high temporal frequencies to capture changes [*Winkley*, 1977; *Hooke*, 1995]. Here we tap into over three decades of global satellite imagery to investigate how cutoff perturbations influence upstream and downstream morphodynamic change along the active tropical Ucayali River in Peru.

2. Methods

We investigated morphodynamic response to 13 cutoffs (Figure 1) using over three decades of Landsat imagery. Annual, bankfull-resolving channel masks were created by compositing individual Landsat scenes

Figure 1. Cutoffs along the Ucayali River. Thirteen cutoff events along the Ucayali River during the period of 1985 to 2015 are shown midway through the cutoff process and at low flow. Chute channels and flow directions are denoted by white arrows. The north arrow and scale bar apply to all images. See Table 1 for more information on the cutoffs.

recorded during low flows. Centerlines and widths were computed for each channel mask using the River Morphodynamics from Analysis of Planforms (RivMAP) toolbox [*Schwenk et al.*, 2016]. Further details regarding mapping and quantifying the Ucayali River's morphodynamic history from Landsat imagery are given in *Schwenk et al*. [2016]. The Ucayali River lies within the Amazon Basin, flowing north along the eastern flank of the Andes Mountains, and together with the Marañon River forms the headwaters of the Amazon River. Among major rivers in the Amazon Basin, the Ucayali's migration pace is second only to the Mamoré River with an average rate of 36 m/yr [*Constantine et al.*, 2014]. The Ucayali's floodplain testifies to its impressive movement with its oxbow lakes, abandoned channels, scroll bars, and sediment splays.

Within the 1985–2015 window of available Landsat imagery of over 1500 km of the Ucayali 42 cutoffs occurred, removing lengths of river ranging from 5 to 89 channel widths. We found an equal number of neck and chute cutoffs (17 of each), and the remaining eight were "tip" cutoffs where the primary flow path bypassed only the apex of the meander bend. Chute cutoffs may span multiple years from initial chute formation to complete bend bypass, and for some cutoffs the meander bends were never completely hydraulically disconnected from the river. In this study, only neck and chute cutoffs that completed within a 2 year

Table 1. Cutoff Locations, Labels, and Properties

Cutoff	Label	Latitude (deg)	Longitude (deg)	Year	Length (km)	Type	Chute Length (km)	Width (m)	Excavated Area (km^2)
Masisea	Ma	−8.511	−74.316	1997	72	chute	7	837	5.3
Tumboya	Tu	−9.883	−74.012	2001	51	chute	8.9	767	6.7
Sampaya 2	S2	−9.550	−74.185	2004	28	neck	2.9	791	0.25
Libertad	Li	−7.240	−75.118	1994	27	neck	7.8	949	0.22
Manchari	Mn	−9.706	−74.127	1998	24	chute	8.6	697	3.3
Iaparia	Ia	−9.242	−74.434	1998	23	neck	1.4	623	0.72
Sampaya 1	S1	−9.566	−74.168	1992	22	chute	2.7	568	2.0
Pucallpa	Pu	−8.348	−74.508	1994	15	chute	2.4	915	0.73
Èxito	Èx	−8.458	−74.434	2002	15	chute	8.1	1020	4.3
San Francisco	Sf	−7.935	−74.935	1999	12	chute	3.2	915	1.6
Tre Unidas	Tr	−8.258	−74.535	2012	11	chute	4.3	769	3.3
Bolognesi	Bo	−10.046	−73.977	2006	9.6	neck	1.5	675	0.29
Bretaña	Br	−5.215	−74.321	2010	8.3	neck	0.67	470	0.13

period and were not near others in space or time were considered so that measured morphodynamic changes were attributable to particular cutoff events. Eight chute cutoffs and five neck cutoffs met these criteria (Figure 1 and Table 1).

2.1. Bend Tracking and Morphodynamic Metrics

We tracked individual meander bends in the vicinity of cutoffs to detect significant planform changes after cutoff occurrence. This approach requires a consistent delineation of each bend through time as the centerline grows and deforms [e.g., *Schwenk et al*., 2015]. Meander bend endpoints were mapped forward and backward in time by minimizing the difference between the point's position, the local centerline angle, and the local centerline curvature to provide smooth endpoint delineations through time. Details and an illustration of our tracking method are provided as supporting information.

Annual centerline migration rates (M_{cl}) were computed for individual meander bends by

$$M_{\mathrm{cl}} = \frac{A_{\mathrm{cl}}}{l_{\mathrm{cl}}(\Delta t)} \tag{1}$$

where A_{cl} is the area traversed by a bend's centerline over period Δt, l_{cl} is the length of the bend's centerline at the beginning of the period, and Δt is 1 year. Average bend widths (W) were computed according to

$$W = \frac{A_b}{l_b} \tag{2}$$

where A_b is the planform area of the bend and l_b is the bend's centerline length.

We used the floodplain erosional net areas as surrogates for estimating the quantity of sediment injected into downstream reaches from floodplain incision during chute channel initiation and development. The mask from the first year before the chute cutoff appeared was subtracted from the mask of the year of complete cutoff. Differenced masks were cropped to the region of cutoff leaving only the floodplain area excavated by the chute channel (A_e).

2.2. Downstream Distance of Cutoff Influence

In order to assess whether a particular cutoff induced morphologic change within a nearby meander bend, precutoff and postcutoff metrics of morphologic change were computed by averaging their values over the 2 years preceding the cutoff (X_{pre}) and 2 years afterward (X_{post}), where X is a metric of a bend's planform morphology—either M_{cl} or W herein. The year of cutoff itself was not included in averaging because the channel planform for that year integrates effects of both precutoff and postcutoff dynamics. Two indices

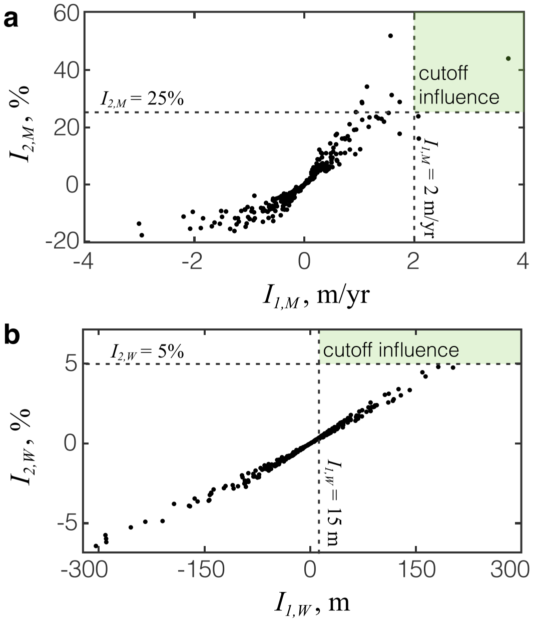

Figure 2. (a and b) Indices of change for bends unaffected by cutoffs. Both indices of change (equation (3)) are computed for 10 meander bends unaffected by cutoffs across 31 years. The indices for migration rates are shown in Figure 2a and for widths in Figure 2b. Our adopted thresholds are shown by dashed lines, and the shaded areas in both plots denote regions of significant cutoff influence where a change in migration rate and/or width falls outside the natural variability. Both plots contain 260 points (10 bends × 26 indices/bend).

were defined to measure the magnitude of cutoff influence by comparing precutoff and postcutoff planforms:

$$I_1 = X_{\text{post}} - X_{\text{pre}} \quad \text{and} \tag{3}$$

$$I_2 = \frac{X_{\text{post}} - X_{\text{pre}}}{X_{\text{pre}}} \times 100\%$$

The first index quantifies the magnitude of change, while the second measures the percent increase or decrease. We estimated the expected ranges of both indices from 10 meander bends unaffected by cutoffs or other local disturbances to set thresholds on I_2 for identifying significant cutoff influence (see Figure 2). The thresholds for I_1 were determined to ensure that identified planform changes exceeded uncertainties inherent in quantifying planform changes from Landsat imagery discussed in *Schwenk et al.* [2016]. Significant cutoff influence on a bend's morphology was inferred if the following thresholds were met: $I_{1,M} \geq 25\%$ and $I_{2,M} \geq 2$ m/yr; $I_{1,W} \geq 5\%$ and $I_{2,W} \geq 15$ m, where $I_{1,M}$ refers to I_1 computed for M_{cl}. In other words, a bend's migration rate was considered to have been significantly affected by cutoffs if its 2 year average increased by at least 25% and 2 m/yr following the cutoff event.

The first bend downstream of each cutoff was tested for significant cutoff influence according to the above conditions. If the bend exhibited cutoff influence, the next downstream bend was tested, and so on until the first bend with no significant influence was reached. The distance of downstream influence of each cutoff on migration rate (D_M) and width (D_W) was defined as the centerline distance from the downstream end of the cutoff reach to the downstream end of the farthest bend that met the above criteria (see Figure 3 for examples of D_M and D_W). It is possible that cutoff effects may propagate further upstream and downstream over times longer than 2 years, so our choice of a 2 year averaging period provides conservative estimates of D_W and D_M.

3. Results

In 1997, the most drastic change in the course of the Ucayali River in over 200 years took place with the cutoff of a human-induced, 72 km triple-lobed meander bend [*Parssinen et al.*, 1996] (Masisea; Figure 1). The cutoff's anthropogenic origins are attributed to local ribereños, who decades earlier in an effort to reduce canoe travel time along the river carved a meter deep by 2 m wide shortcut channel across the neck of the Masisea bend. Modest efforts in the 1980s to enlarge the channel culminated in the use of a tractor to widen its entrance, and the Ucayali commandeered the tiny channel during the following 1997 flooding season [*Abizaid*, 2005]. The river's dramatic morphodynamic response to the Masisea cutoff is evident from the changes in upstream and downstream bend migration rates and widths following the cutoff (Figure 3). In the downstream direction, bends D1–D8 migrated 95–466% faster and D1–D4 widened 11–26% after the cutoff occurred. Upstream of the Masisea cutoff, three small-amplitude, downstream-translating bends (U1–U3) sustained accelerated migration (80–204% faster) and widening (19–27% wider) following the

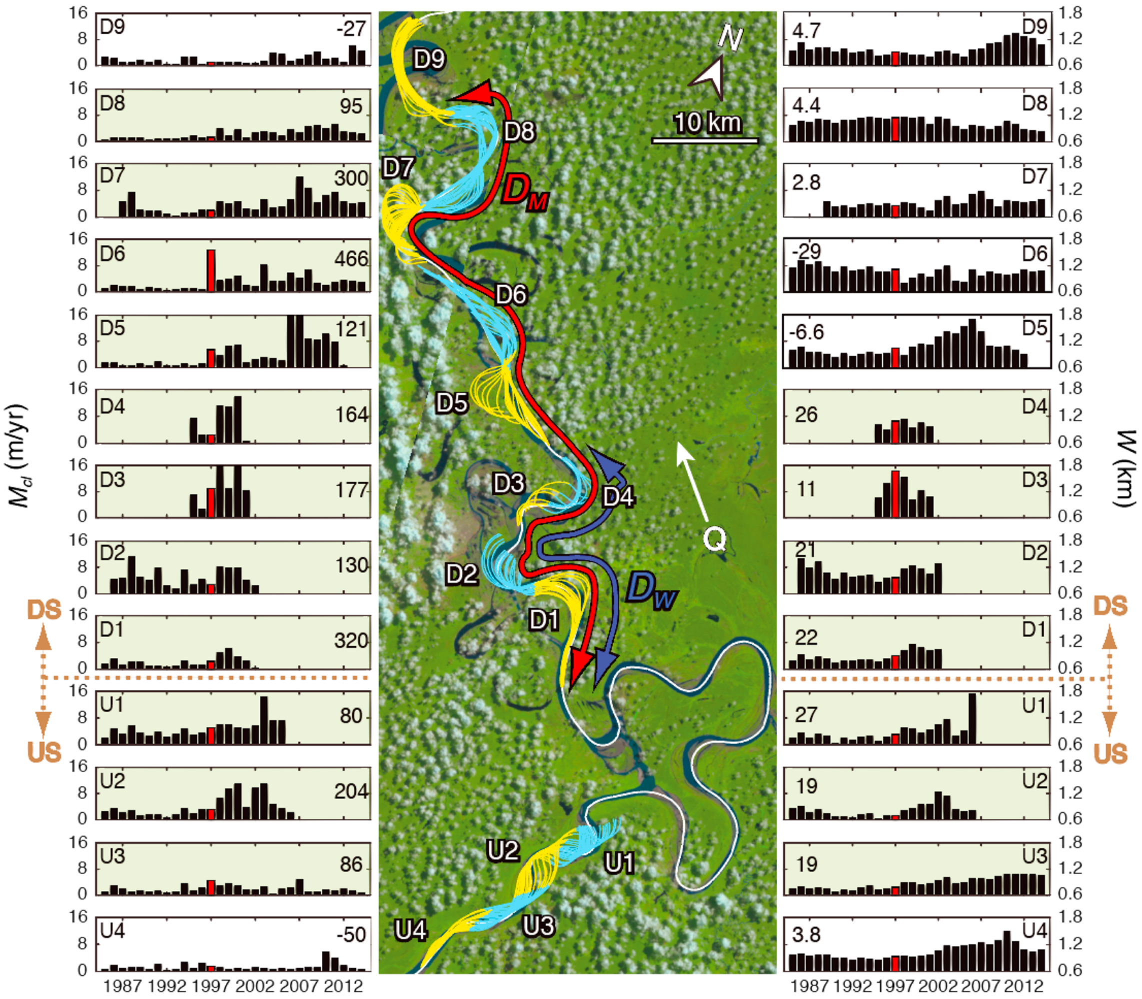

Figure 3. Response of bends near the Masisea cutoff. (left column) Migration rates (M_{cl}) and (right column) widths (W) for individual bends near the Masisea cutoff are plotted through time. The red bars highlight 1997, the year of the Masisea cutoff. The numbers in each plot show the I_2 value (2 year % increase) for each bend. Bends surpassing the thresholds for significant cutoff influence are shaded green. (middle column) Locations of four upstream (U1–U4) and nine downstream (D1–D9) bends are shown, with the 1997 centerline shown in white. The downstream distances of accelerated migration (D_M, red) and widening (D_W, blue) for the Masisea cutoff are shown.

cutoff. Morphodynamic changes due to the Masisea cutoff spurred the eventual cutoff of bends U1, D1, D4, and D5, while bends downstream of the Masisea cutoff that had not yet cut off (i.e. D6-D9) exhibited elevated migration rates sustained for over a decade following the cutoff. Similarly, the upstream bends U3 and U4 underwent persistent widening following the cutoff.

To ensure that the Masisea cutoff was indeed the driver of morphodynamic change rather than an effect of external forcings such as changes in hydrology, floodplain heterogeneity, or sediment load, 12 additional cutoffs along the Ucayali River were also considered (see Figure 1 and Table 1). The cutoffs were separated by sufficient distance and/or time to ensure that their influences on channel morphodynamics were independent of each other. The Èxito (Èx) cutoff (bend D1 in Figure 3) is the lone exception; it was immediately downstream of and occurred only 5 years after the Masisea cutoff, and its influence on the Ucayali's morphodynamics may be conflated with a sustained response to the Masisea event.

Meander bends downstream of cutoffs migrated at least 25% more rapidly after cutoff at 11 of 13 sites (Figure 4a), and a regression between D_M and the change in river length following cutoff (ΔL) indicates a linear scaling between the downstream extent of accelerated migration due to cutoff with the net change in river length after cutoff. Migration rates for the first downstream bends at the two sites "Mn" and "Tr" with no significant downstream influence (i.e., $D_M = 0$) did increase by 10% and 15%, respectively, but these values did not exceed the 25% threshold. No significant relationship was found between the excavated area (A_e) and D_M, indicating that although sediment pulses due to floodplain excavation during cutoff may promote morphodynamic change, they did not control the spatial extent of accelerated migration. Modest channel straightening at neck cutoffs contributed to their small but nonzero excavated areas, but overall, neck cutoffs reworked smaller floodplain areas than chute cutoffs. Significant downstream channel widening after cutoffs occurred at 8 of 13 sites (Figures 4b and 4c). The downstream extent of cutoff-induced channel widening (D_W) showed similar dependence on both the length of channel removed by cutoff ($r^2 = 0.70$) and the excavated area ($r^2 = 0.65$). Regressions in Figure 4 were forced through the origin based on physical reasoning that a significant morphodynamic response cannot occur in the absence of a cutoff. The fitted linear relationships depend significantly on the “Ma” and “Tu” cutoffs although removal of these points barely altered the slope of the regression in Figure 4a. For trends reported in Figures 4b and 4c, removal of Ma and Tu resulted in 27 and 38% decreases in the slopes, but the slopes of all regressions, including those excluding Ma and T′, were significantly different from zero at the 95% confidence level.

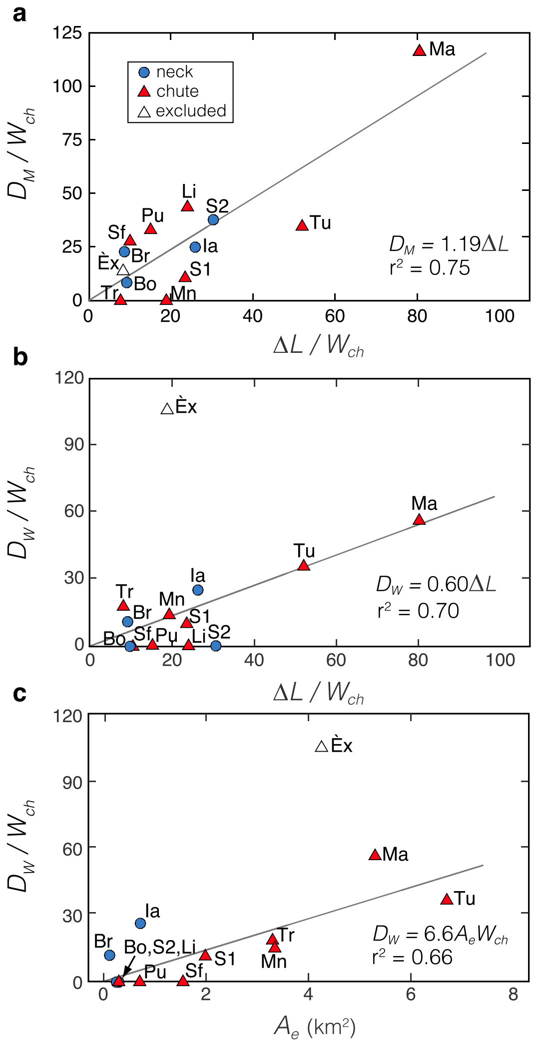

Figure 4. The influence of cutoffs on downstream morphodynamic change. (a) The downstream distance of accelerated migration (D_M) is plotted against the change in river length due to cutoff (ΔL); both quantities are normalized by the average width of the Ucayali River ($W_{ch} = 825$ m). (b) The normalized downstream distance of channel widening (D_W/W_{ch}) is plotted against the normalized change in river length due to cutoff ($\Delta L/W_{ch}$). (c) The normalized downstream distance of channel widening (D_W/W_{ch}) is plotted against the normalized area of excavated floodplain (A_e/W_{ch}^2). The Èxito cutoff (Èx) was excluded from regressions due to its proximity in space and time to the Masisea cutoff.

Figure 4 also provides insight into the Ucayali’s preferential modes of self-adjustment following cutoff perturbations. With the exception of the downstream-translating U1–U3 bends at Masisea and a handful of devolving bends, centerline migration corresponded to bend elongation [*Schwenk et al.*, 2016]. River response via elongation (10/12 cutoffs) occurred more frequently than widening (7/12 cutoffs). The spatial extent of cutoff-induced elongation (D_M) was greater than the extent of channel widening (D_W) for seven cutoffs and equal for three cutoffs. Only for two cutoffs was cutoff-induced channel widening observed farther downstream than accelerated migration. The slopes of the regressions in Figures 4a and 4d also indicate that on average, the downstream distance of cutoff-accelerated migration (D_M) is roughly twice that of cutoff-induced channel widening (D_W).

4. Discussion

The physical mechanisms responsible for channel widening and accelerated migration following cutoffs are not immediately discernable from planform dynamics alone, but channel migration in the Ucayali is driven primarily by its sediment load [*Constantine et al*., 2014; *Schwenk et al*., 2016], and enhanced downstream sediment flux due to cutoff may account for the bulk of accelerated migration and bend widening. Although initial pulses of sediment due to chute formation do not explain the spatial extents of accelerated migration, diffusion of the locally steep bed elevation following cutoff may result in a more continuous sediment supply over a longer time period [*Winkley*, 1977; *Biedenharn et al*., 2000]. Similar effects have also been documented in artificially straightened channels [*Parker and Andres*, 1976; *Simon and Robbins*, 1987]. Changes in slope are typically the initially dominant morphodynamic response to cutoffs in alluvial rivers and may cause an immediate backwater effect upstream of the cutoff [see *Lane*, 1947] (Figure 1). As the slope perturbation diffuses upstream and downstream over a period of years, the upstream bed scours, releasing sediment to the downstream reach which may drive morphodynamic change [*Lane*, 1947] and sustain accelerated migration rates as observed near the Masisea cutoff. If a graded reach of river with length l_o and elevation loss ΔE undergoes a cutoff that removes ΔL of river length, its change in slope (ΔS) is given by

$$\Delta S = \frac{\Delta E \Delta L}{l_o(l_o - \Delta L)}. \tag{4}$$

If the reach under consideration is significantly longer than the change in river length due to cutoff (i.e., $l_o >> \Delta L$), then

$$\Delta S \approx \frac{\Delta E \Delta L}{l_o^2} \tag{5}$$

indicating that the magnitude of the slope perturbation following cutoff is proportional to the length of removed river (ΔL).

In addition to sediment released from the upstream bed during reestablishment of an equilibrium slope, the reach immediately downstream may also receive larger water and sediment loads relative to precutoff conditions due to the river's loss of floodplain storage and/or synchronization with local sources, e.g., tributaries [*Lane*, 1947]. The magnitude of the loss of storage depends on local floodplain topography, flow conditions, and channel geometry but for a uniform floodplain scales with ΔL. Thus, ΔL estimates both the magnitude of bed slope perturbations and lost floodplain storage following cutoffs and accounts for 75% ($r^2 = 0.75$) of the variation of the downstream distance of cutoff influence D_M for 12 cutoffs in the Ucayali River.

The nonlocal acceleration of planform change of the Ucayali cutoffs, and in particular the response to the Masisea cutoff, provides perhaps the strongest support yet for considering meandering river planform dynamics as self-organized critical (SOC) systems that maintain critical stable states [*Stolum*, 1996, 1997; *Hooke*, 2004]. The classic SOC system is the rice pile, which maintains a critical slope at which point adding a single grain may result in clusters of avalanches. Previous studies have found power law scaling, a feature of SOC systems, in cutoff clusters from numerical models of long-time meander evolution [*Stolum*, 1996, 1997] and cutoff clusters in real rivers over short time periods [*Hooke*, 2004]. Clustering of cutoff events implies that an initial cutoff event is likely to induce further cutoffs nearby, a response requiring (1) available bends to cutoff (high sinuosity) and (2) a nonlocal influence of cutoffs. While highly sinuous meandering rivers are not uncommon, our results provide the first evidence linking cutoff events to nonlocal morphodynamic change required to initiate and sustain SOC-type avalanching. Cutoff rates were shown to scale exponentially with migration rates for tropical Amazonian rivers [*Constantine et al*., 2014], indicating that the observed nonlocal accelerated migration due to cutoffs in the Ucayali River increased the likelihood of further cutoffs. Accelerated migration and four cutoffs occurring near and after the Masisea cutoff (bends U1, D1, D4, and D5) exemplified such avalanching dynamics.

Current long-time numerical models of meander migration driven by centerline curvature cannot reproduce the cutoff-induced nonlocal accelerated morphodynamics in the Ucayali River. Although local migration rates do depend nonlocally on curvature through a convolution integral [*Ikeda et al*., 1981; *Howard and Knutson*, 1984], the distance of influence is usually negligible beyond a single meander bend in models [*Sun et al*., 2001]. The same has been shown empirically in some natural channels [*Güneralp and Rhoads*, 2009]. Models may predict nonlocal accelerated migration rates following cutoff due to the creation of localized spikes in centerline curvature at the cutoff location [e.g., *Schwenk et al*. [2015]]. However, the Ucayali River showed that even cutoffs that do not result in locally high curvature may still drive nonlocal accelerated migration (e.g., see Li, Èx, Bo, and Ia in Figures 1 and 4), implying that curvature alone cannot account for the processes responsible for accelerated nonlocal morphodynamic change. In the absence of these physics, the avalanching behavior apparent from current meandering models cannot arise from internal system dynamics but is instead the result of geometric constraints on meander topology.

5. Conclusions

Cutoffs play a vital and controlling role on the long-term planform dynamics of migrating rivers. Our results establish cutoffs as morphodynamic perturbations with nonlocal influence and present new modeling and theoretical challenges. Based on 13 independent cutoffs along the Ucayali River, our analysis suggests that downstream changes are primarily driven by sediment fluxes initiated by gradient adjustments and/or chute channel excavations associated with cutoffs. The mechanisms responsible for upstream responses to cutoffs are less clear but may be influenced by a backwater effect. Current long-time models of meandering river dynamics lack the mechanisms to account for gradient adjustments and spatial variations in sediment loads, but our results suggest these processes are critical for capturing morphodynamic response to cutoffs, calling for experimentation, field studies, and detailed numerical modeling aimed at improving the mechanisms responsible for nonlocal morphodynamic changes.

Our results also reveal how the Ucayali River “authored its own geometry” [*Leopold and Langbein*, 1962] through planform adjustments following cutoffs. These insights, made possible through Landsat imagery recorded at high temporal frequency, demonstrate the vast potential of satellite imagery to advance our understanding of river morphodynamics in response to human and natural influences. The Masisea cutoff avalanche demonstrates how seemingly insignificant local human activity can have unintended and far-reaching impacts on the livelihoods of millions of Peruvians who rely on the Ucayali River for economic and transportation benefits. Other major Amazonian rivers facing extensive damming [*Finer and Jenkins*, 2012], expanding mining activity [*Asner et al*., 2013], and accelerating deforestation [*Fearnside*, 2015] demand a deeper understanding of how river morphodynamics respond to perturbations, and our results show how even natural perturbations can spur dramatic and widespread changes.

Acknowledgments
This research benefitted from collaborations made possible through Linked Institutions for Future Earth funded under NSF’s Science Across Virtual Institutes program (NSF grant EAR-1242458). Funding was also provided by NSF grant EAR-1209402 under the Water Sustainability and Climate Program: REsilience under Accelerated CHange. We thank Hans-Henrik Stølum for fruitful discussion while developing the manuscript and Bruce Rhoads and Jessica Leroy for insightful and constructive reviews. J.S. acknowledges support provided by an NSF Graduate Research Fellowship. Ankush Khandelwal, Eric McCaleb, Mace Blank, and Anuj Karpatne of the University of Minnesota’s Computer Science Department provided assistance obtaining and classifying Landsat imagery of the Ucayali River. Landsat imagery was acquired from the Google Earth Engine API, and Mulu Fratkin assisted with quality control and processing using the RivMAP toolbox to quantify planform changes, which is available at https://www.mathworks.com/matlabcentral/fileexchange/58264-rivmap-river-morphodynamics-from-analysis-of-planforms.

References

Abizaid, C. (2005), An anthropogenic meander cutoff along the Ucayali River, Peruvian Amazon, *Geogr. Rev.*, *95*(1), 122–135.

Asner, G. P., W. Llactayo, R. Tupayachi, and E. R. Luna (2013), Elevated rates of gold mining in the Amazon revealed through high-resolution monitoring, *Proc. Natl. Acad. Sci. U.S.A.*, *110*(46), 18,454–18,459, doi:10.1073/pnas.1318271110.

Biedenharn, D. S., C. R. Thorne, and C. C. Watson (2000), Recent morphological evolution of the Lower Mississippi River, *Geomorphology*, *34*, 227–249, doi:10.1016/S0169-555X(00)00011-8.

Camporeale, C., E. Perucca, and L. Ridolfi (2008), Significance of cutoff in meandering river dynamics, *J. Geophys. Res.*, *113*, F01001, doi:10.1029/2006JF000694.

Constantine, J. A., T. Dunne, J. Ahmed, C. J. Legleiter, and E. D. Lazarus (2014), Sediment supply as a driver of river meandering and floodplain evolution in the Amazon Basin, *Nat. Geosci.*, *7*(12), 899–903, doi:10.1038/ngeo2282.

Eekhout, J. P. C., and A. J. F. Hoitink (2015), Chute cutoff as a morphological response to stream reconstruction: The possible role of backwater, *Water Resour. Res.*, *51*, 3339–3352, doi:10.1002/2014WR016539.

Fearnside, P. M. (2015), Environment: Deforestation soars in the Amazon, *Nature*, *521*(7553), 423–423, doi:10.1038/521423b.

Finer, M., and C. N. Jenkins (2012), Proliferation of hydroelectric dams in the Andean Amazon and implications for Andes-Amazon connectivity, *PLoS One*, *7*(4), 1–9, doi:10.1371/journal.pone.0035126.

Fisk, H. N., P. R. Mabrey, J. W. B. Steinriede, A. Osanik, and W. J. Turnbull (1949), *Geological Investigation of Mississippi River Acitivity: Memphis, Tennessee, to Mouth of Arkansas River*, U.S. Army Corp of Engineers Technical Memorandum (USACE), Vickburg, Miss.

Fuller, I. C., A. R. G. Large, and D. J. Milan (2003), Quantifying channel development and sediment transfer following chute cutoff in a wandering gravel-bed river, *Geomorphology*, *54*, 307–323, doi:10.1016/S0169-555X(02)00374-4.

Grenfell, M. C., A. P. Nicholas, and R. Aalto (2014), Mediative adjustment of river dynamics: The role of chute channels in tropical sand-bed meandering rivers, *Sediment. Geol.*, *301*, 93–106, doi:10.1016/j.sedgeo.2013.06.007.

Güneralp, I., and B. L. Rhoads (2009), Empirical analysis of the planform curvature-migration relation of meandering rivers, *Water Resour. Res.*, *45*, W09424, doi:10.1029/2008WR007533.

Hooke, J. M. (1995), River channel adjustment to meander cutoffs on the River Bollin and River Dane, northwest England, *Geomorphology*, *14*(3), 235–253, doi:10.1016/0169-555X(95)00110-Q.

Hooke, J. M. (2004), Cutoffs galore!: Occurrence and causes of multiple cutoffs on a meandering river, *Geomorphology*, *61*, 225–238, doi:10.1016/j.geomorph.2003.12.006.

Howard, A. D., and T. R. T. Knutson (1984), Sufficient conditions for river meandering: A simulation approach, *Water Resour. Res.*, *20*(11), 1659–1667, doi:10.1029/WR020i011p01659.

Hudson, P. F., and R. H. Kesel (2000), Channel migration and meander-bend curvature in the lower Mississippi River prior to major human modification, *Geology*, *28*(6), 531–534, doi:10.1130/0091-7613(2000)28<531:CMAMCI>2.0.CO;2.

Ikeda, S., G. Parker, and K. Sawai (1981), Bend theory of river meanders. Part 1. Linear development, *J. Fluid Mech.*, *112*, 363–377, doi:10.1017/s0022112081000451.

Jugaru Tiron, L., J. Le Coz, M. Provansal, N. Panin, G. Raccasi, G. Dramais, and P. Dussouillez (2009), Flow and sediment processes in a cutoff meander of the Danube Delta during episodic flooding, *Geomorphology*, *106*, 186–197, doi:10.1016/j.geomorph.2008.10.016.

Lane, E. W. (1947), The effect of cutting off bends in rivers, in *Proceedings of the Third Hydraulics Conference*, pp. 230–240, Univ. of Iowa Studies in Engineering, Iowa City, Iowa.

Leopold, L. B., and W. B. Langbein (1962), *The Concept of Entropy in Landscape Evolution*, AGU, Washington, D. C.

Micheli, E. R., and E. W. Larsen (2011), River channel cutoff dynamics, Sacramento river, California, USA, *River Res. Appl.*, *344*(27), 328–344, doi:10.1002/rra.1360.

Parker, G., and D. Andres (1976), Detrimental effects of river channelization, *Proc. Conf. Rivers*, *76*, 1248–1266.

Parssinen, M., J. Salo, and M. Rasanen (1996), River floodplain relocations and the abandonment of aborigine settlements in the Upper Amazon basin: A historical case study of San Miguel de Cunibos at the Middle Ucayali River, *Geoarchaeology*, *11*(4), 345–359, doi:10.1002/(SICI)1520-6548(199607)11:4<345::AID-GEA3>3.0.CO;2-1.

Schwendel, A. C., A. P. Nicholas, R. Aalto, G. H. Sambrook Smith, and S. Buckley (2015), Interaction between meander dynamics and floodplain heterogeneity in a large tropical sand-bed river: The Rio Beni, Bolivian Amazon, *Earth Surf. Processes Landforms*, *40*(15), 2026–2040, doi:10.1002/esp.3777.

Schwenk, J., S. Lanzoni, and E. Foufoula-Georgiou (2015), The life of a meander bend: Connecting shape and dynamics via analysis of a numerical model, *J. Geophys. Res. Earth Surf.*, *120*, 690–710, doi:10.1002/2014JF003252.

Schwenk, J., A. Khandelwal, M. Fratkin, V. Kumar, and E. Foufoula-Georgiou (2016), High spatio-temporal resolution of river planform dynamics from Landsat: The RivMAP toolbox and results from the Ucayali River, *Earth Space Sci.*, doi:10.1002/2016EA000196.

Simon, A., and C. H. Robbins (1987), Man-induced gradient adjustment of the South Fork Forked Deer River, west Tennessee, *Environ. Geol. Water Sci.*, *9*(2), 109–118, doi:10.1007/BF02449942.

Słowik, M. (2016), The influence of meander bend evolution on the formation of multiple cutoffs: Findings inferred from floodplain architecture and bend geometry, *Earth Surf. Processes Landforms*, *41*(5), 626–641, doi:10.1002/esp.3851.

Stolum, H.-H. (1996), River meandering as a self-organization process, *Science*, *271*(5256), 1710–1713, doi:10.1126/science.271.5256.1710.

Stolum, H.-H. (1997), Fluctuations at the self-organized critical state, *Phys. Rev. E*, *56*(6), 6710–6718, doi:10.1103/physreve.56.6710.

Sun, T., P. Meakin, and T. Jøssang (2001), A computer model for meandering rivers with multiple bed load sediment sizes: 2. Computer simulations, *Water Resour. Res.*, *37*(8), 2243–2258, doi:10.1029/2000WR900396.

Winkley, B. R. (1977), Man-made cutoffs on the Lower Mississippi River, conception, construction, and river response, *Potamology Invest.*, 1–219.

Zinger, J. A., B. L. Rhoads, and J. L. Best (2011), Extreme sediment pulses generated by bend cutoffs along a large meandering river, *Nat. Geosci.*, *4*(10), 675–678, doi:10.1038/ngeo1260.

Zinger, J. A., B. L. Rhoads, J. L. Best, and K. K. Johnson (2013), Flow structure and channel morphodynamics of meander bend chute cutoffs: A case study of the Wabash River, USA, *J. Geophys. Res. Earth Surf.*, *118*, 2468–2487, doi:10.1002/jgrf.20155.